Макрогетероциклы
http://mhc-isuct.ru

DOI: 10.6060/mhc245927p

Cu 5,10,15,20-Tetrakis(3-aminophenyl)porphyrin Films Obtained via Polymerization Using Electrooxidation or Superoxide Assistance as Initiating Step

Vladimir I. Parfenyuk, Sergey M. Kuzmin,[@] Svetlana A. Chulovskaya, and Yuliya A. Filimonova

G.A. Krestov Institute of Solution Chemistry, Russian Academy of Sciences, 153045 Ivanovo, Russia
[@]Corresponding author E-mail: smk@isc-ras.ru

Dedicated to the great scientist and science organizer O. I. Koifman

It was shown that the electropolymerization of Cu 5,10,15,20-tetrakis(3-aminophenyl)porphyrin from dimethyl sulfoxide can be carried out both by electrochemical oxidation of the porphyrin, and via initiating the process with electrochemically synthesized superoxide. In oxygenated solutions, initiation of polymerization by superoxide provides a greater contribution to a film formation than electrochemical oxidation of porphyrin. The rates of the film formation by these two mechanisms differ by approximately three times. Despite the differences in the rate of formation and surface morphology of the films for oxygen-free and oxygen-saturated solutions, the resulting materials' surface is formed by particles of similar lateral sizes. The resulting roughness also differs insignificantly. This indicates a proportional increase in both the rate of nucleation and the rate of new phase growth in the presence of oxygen. The long-wavelength absorption edge of the semiconductor material is revealed in the short-wavelength region of the UV-Vis film spectrum. The calculation resulted in the band gap values of 3.48 and 3.19 eV for materials obtained by porphyrin oxidation and via the superoxide assistance, respectively. The influence of the obtaining method of the Cu 5,10,15,20-tetrakis(3-aminophenyl)porphyrin-based material on the reaction of the electro-reduction of oxygen on its surface in an alkaline medium was shown.

Keywords: Porphyrin, electropolymerization, mechanism, films, surface, band gap value, oxygen reduction reaction.

Пленки Cu 5,10,15,20-тетракис(3-аминофенил)порфирина при инициировании полимеризации электрохимическим окислением и супероксидом в качестве медиатора

В. И. Парфенюк, С. М. Кузьмин,[@] С. А. Чуловская, Ю. А. Филимонова

Институт химии растворов им. Г.А. Крестова Российской академии наук, 153045 Иваново, Россия
[@]E-mail: smk@isc-ras.ru

О. И. Койфману – большому ученому и организатору науки посвящается

Показано, что электрополимеризация Cu 5,10,15,20-тетракис(3-аминофенил)порфирина из растворов в диметилсульфоксиде может быть осуществлена как при электрохимическом окислении порфирина, так и при инициировании процесса электрохимически синтезируемым супероксидом. В насыщенных кислородом растворах инициирование полимеризации супероксидом дает больший вклад в формирование пленки, чем электрохимическое окисление порфирина; скорости формирования пленки по этим механизмам различаются приблизительно в три раза. Несмотря на различия скорости формирования и морфологии поверхности пленок, наблюдающихся в бескислородных и насыщенных кислородом растворах, поверхность полученных материалов сформирована частицами близкого латерального размера. Несущественно различаются и шероховатости поверхностей частиц. Это указывает на пропорциональное повышение в присутствии кислорода, как скорости зародышеобразования, так и скорости роста новой фазы. Анализ коротковолновой области спектра пленок демонстрирует длинноволновую границу поглощения полупроводникового

материала. Расчет приводит к величинам ширины запрещенной зоны около 3.48 и 3.19 эВ для материалов, полученных окислением порфирина и медиаторным способом, соответственно. Показано влияние способа получения материала на основе Cu 5,10,15,20-тетракис(3-аминофенил)порфирина на реакцию электровосстановления кислорода в щелочной среде на его поверхности.

Ключевые слова: Порфирин, электрополимеризация, механизм, пленки, поверхность, ширина запрещенной зоны, реакция восстановления кислорода.

Introduction

Due to their complexing, redox and photophysical properties, compounds of the porphyrin series attract close attention as parent molecular structures for creation of catalytic, photovoltaic and sensor systems.[1-10] As a rule, the key element of the above-mentioned devices is the active layer, in which porphyrin molecules are assembled into supramolecular structures in a certain way.[11-13] When the active layer of a device is located on a conductive substrate, the electrochemical methods turn out to be a convenient tool for its preparing.[14-16] In this respect, polymer active layers[15-16] obtained by electropolymerization[14,15] or copolymerization[17-20] of porphyrins are attractive for creating such devices. Electrochemical approaches to the formation of polymer film materials combine the simplicity of technological equipment, and the low costs, with the ample opportunities for monitoring and control of the technological process.[21,22] The work[23] shows that change of environment, from which the electrochemical deposition of the polyporphyrin occurs, results in changing: a) the porphyrin electrochemical behavior; b) film deposition rate; c) size of the deposited particles and aggregates; d) chromophore state in the formed material; e) morphological characteristics of the material surface. We have also demonstrated the influence of the amino group position in the phenyl substituent and substrate material on the porphyrin electrochemical behavior and deposited film properties. Potential scan rate variations in the process of electrochemical deposition of poly-aminophenylporphyrin films in potentiodynamic conditions change the surface morphology and efficiency of material formation.[24] When the growth efficiency is low, they lead to the formation of films with a rather smooth surface; when it is high, the film surface resembles "crumpled paper". This allows scan rate to be considered as a control parameter when the surface morphology significantly affects the film functional characteristics.

In the present work, we investigate the processes of formation of polyporphyrin films via two polymerization mechanisms, in particular, the initiated by the oxidation of porphyrin, and initiated by the interaction of porphyrin with superoxide. The possibility of deposition of aminophenylporphyrins' films from dimethyl sulfoxide when the process is activated by an electrochemically synthesized superoxide anion radical ($O_2^{\bullet -}$) was shown earlier elsewhere.[15,25] For electropolymerized films based on aminophenylporphyrins, the type of porphyrin fragments' binding in the polymer chain was determined;[26] and the prospects for their use as sensors,[27,28] catalysts,[10,29] and nonlinear optical devices[30] were shown. The object of the present study is Cu 5,10,15,20-tetrakis(3-aminophenyl)porphyrin. During its' film formation from dimethyl sulfoxide solutions, the mechanism of superoxide-initiated polymerization both can be turned "on" and "off." Here we compare the physicochemical and practical characteristics of films obtained via two mentioned mechanisms.

Experimental

Synthesis

2H-5,10,15,20-Tetrakis(3-aminophenyl)porphyrin (H_2T(3-NH_2Ph)P) was synthesized using a two-step procedure. At the first stage, 5,10,15,20-tetrakis(3-nitrophenyl)porphyrin was obtained as a result of the reaction of pyrrole with 3-nitrobenzaldehyde. At the second stage, the intermediate product was reduced to H_2T(3-NH_2Ph)P according to the procedure described earlier.[31]

To prepare *Cu 5,10,15,20-tetrakis(3-aminophenyl)porphyrin* (CuT(3-NH_2Ph)P), a solution containing H_2T(3-NH_2Ph)P (0.15 mmol) and copper chloride excess ($CuCl_2$, about 0.8 mmol) in 10 mL of DMF was boiled for 1 h. The reaction mixture was poured into 100 mL of water. The residue was filtered with water and dried in air. Then, the residue was dissolved in a mixture of 100 mL of water and 1.5 mL of concentrated HCl. The undissolved residue was filtered off; the filtrate was neutralized with 25% ammonia solution; the precipitate was filtered and dried in air at room temperature. The formation of CuT(3- NH_2Ph)P (Figure 1) was confirmed by optical spectra with typical Q-band position (Figure 3a, curve 1).

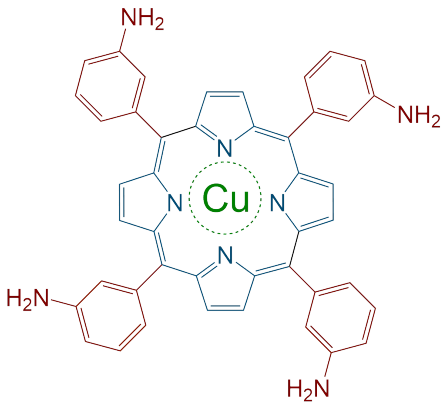

Figure 1. Structure of the porphyrin under study.

Electrochemical procedure

Electrochemical studies were performed on an SP-150 potentiostat (Bio-Logic Science Instruments, France). The deposition of polyporphyrin films was carried out in a three-electrode electrochemical cell from $1 \cdot 10^{-3}$ M solutions of CuT(3-NH_2Ph)P in a DMSO solution (DMSO > 99.5%, Aldrich). A 0.02 M tetrabutylammonium perchlorate(TBAP > 99.0, Aldrich) was used as a supporting electrolyte. Fluorine-doped tin oxide electrode (FTO, KV-FTO-R15T22-100100, Sheet Resistance < 15 ohm/sq, Trans-

mittance > 83%) was used as the working electrode. The working electrode potential was set in relation to the Hg/Hg_2C_{l2} (1 M LiCl) reference electrode using a Luggin capillary. A disk of platinized platinum of 25 mm was an auxiliary electrode located at a distance of 5 mm from the working electrode. To turn “off” the mechanism of superoxide-initiated polymerization, the dissolved oxygen was removed from solutions by Ar (99.998%) bubbling for 30 minutes before film deposition. The method used in the present study for film formation was sufficiently effective. Films formed under these conditions are marked as "Film **I**". To switch “on” the superoxide-initiated polymerization, oxygen (99.7%) was bubbled for 30 min into the solution before film deposition. Films obtained under these conditions are marked as "Film **II**". The films were formed by cycling the working electrode potential in the range from -2.0 to +1.5 V with scan rate of 20 mV/s for 10 cycles. The resulting film was removed from the electrochemical cell, washed with pure DMSO, and dried in ambient conditions for 24 h.

The spectra of solutions of porphyrins in DMSO and their films on FTO electrodes were recorded in a 1 cm quartz cuvette on a Cary 50 spectrometer (Varian, USA). The spectrum of a cuvette filled with DMSO was used as a baseline when studying solutions. When studying films, the spectrum of a cuvette filled with DMSO with a clean FTO electrode placed in it was used. The morphology of the film surface was studied by atomic force electron microscopy using a Solver-47-Pro microscope (NT-MDT, Russia).

To evaluate the electrochemical response of the oxygen electroreduction reaction (ORR), films were deposited on a carbositall electrode. The study was performed on rotating at a speed of 500 rpm electrode in thermostated (25 ± 0.5 °C) oxygen-saturated 0.1 M KOH solution. The potential of the working electrode was set in relation to the Ag/AgCl (3.5 M KCl) reference electrode; the auxiliary electrode was a glassy carbon rod of 4 mm in diameter. Linear voltammograms (LSV) were recorded in the range from 0.0 V to -0.8 V with a potential sweep rate of 10 mV/s.

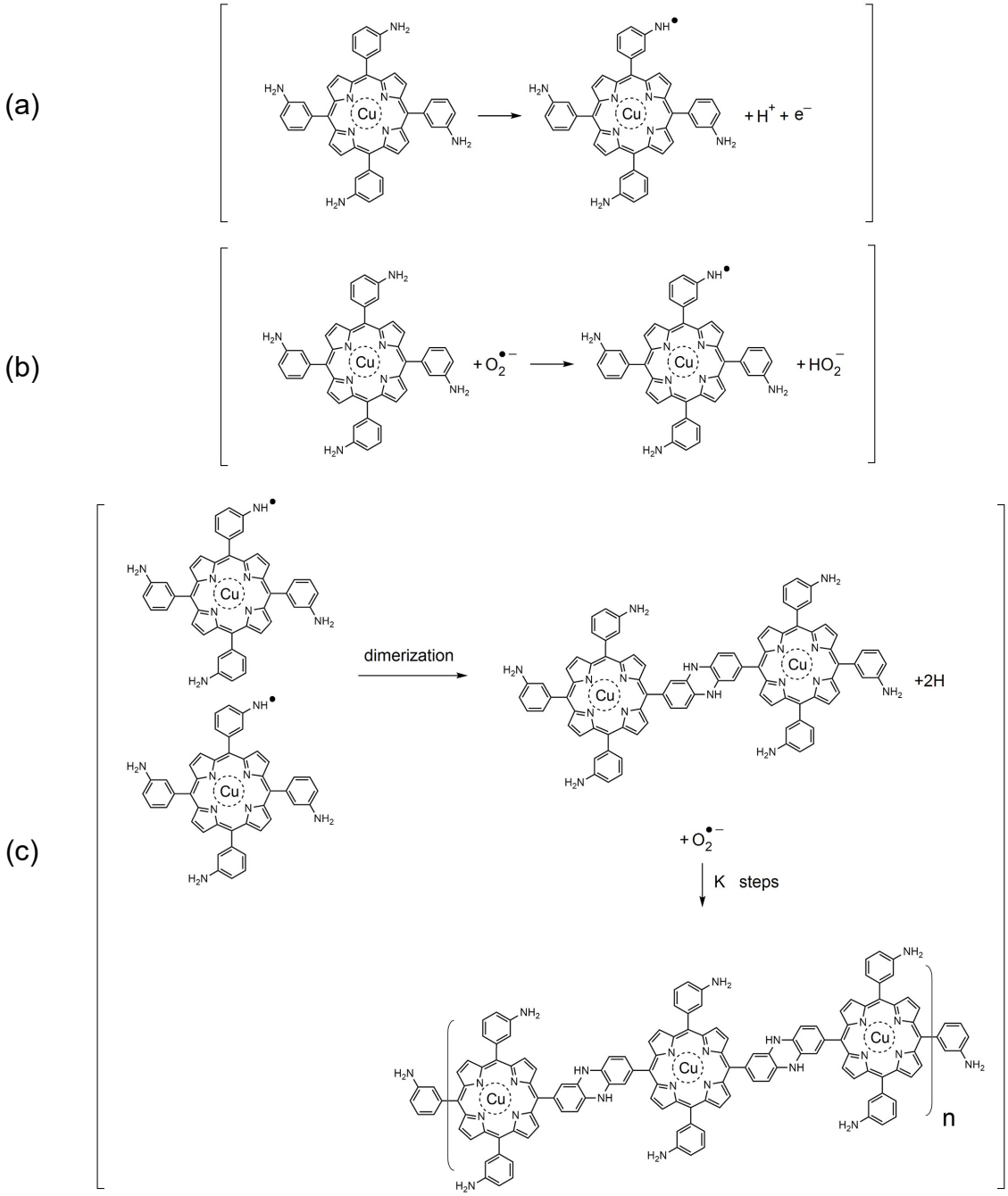

Scheme 1. Formation of radical forms of porphyrin during electrooxidation (a) and during the interaction of porphyrin with superoxide (b); formation of a dimer (hereinafter referred to as a polymer chain) during the recombination of radicals (c).

Results and Discussion

Film formation

Figure 2a shows that in oxygen-free DMSO solutions on the FTO electrode the Faraday processes are not observed in the range from -2.0 to +1.5 V (see curve 1). In $1 \cdot 10^{-3}$ M CuT(3-NH_2Ph)P solution, electrochemical responses of porphyrin reduction are observed in the first cycle (current maxima at potentials of about -1.27 V and -1.79 V, Figure 2b, thick line). These maxima have complementary responses from the oxidation of reduced forms of porphyrin (current maxima at potentials of about -1.17 V and -1.67 V). In the positive potential region, no irreversible response of porphyrin oxidation is observed (maximum current at a potential of 1.18 V). The value of current of the porphyrin electrooxidation peak is approximately two times greater than the value of current of the electroreduction peak. It can be assumed that the porphyrin reduction processes are one-electron, and are represented with the redox transformations of the metal ion Cu^{2+}/Cu^{+} and Cu^{+}/Cu^{0}. And the electrooxidation involves the transfer of two electrons. Electrooxidation is accompanied by deprotonation of porphyrin with the radical forms formation (Scheme 1a). The recombination of these radical forms leads to the formation of a polymer (Scheme 1c). The formation of phenazine-like bridges as the main type of binding of aminophenylporphyrins was demonstrated in the following literature sources.[32,33] The proposed scheme demonstrates the type of binding between the porphyrin fragments in the polymer chain, but does not reflect the polymer molecular structure. Such reactions occurrence is indicated by the appearance of new electrochemical responses (electroreduction at about -0.98 V and electrooxidation at about +0.83 V). The value of current of these new responses increases from cycle to cycle. The formation of Film **I** on the surface of the FTO electrode is observed visually (Figure 2b, inset). The possible types of bridges between porphyrins during polymer formation via the electrochemical oxidation of aminophenylporphyrins were previously described elsewhere.[26]

Just like in an oxygen-free environment, in solutions saturated with oxygen the presence of porphyrin significantly changes the CV curve (Figure 2a, curve 2, and 2c). The electroreduction of oxygen in DMSO (Figure 2a) occurs via a one-electron mechanism with the formation of a superoxide anion-radical stable in DMSO solutions.[34,35] The adsorption of porphyrin on the electrode changes the electron transfer parameters across the interface. This leads to the current maxima shift and their magnitude change (Figure 2 a,c). An electroreduction response near +1.0 V appears, which may indicate the appearance of metallo-porphyrin and superoxide adducts. Superoxide is a good hydrogen atom acceptor, thus the transfer of a labile hydrogen atom from the aminophenyl substituent to the superoxide is possible (Scheme 1b). This reaction leads to the appearance of radical forms of porphyrin,[25] which under recombination result in formation of a polyporphyrin film (Scheme 1c). The Film **II** growth is accompanied by a change in the CV curve from cycle to cycle (Figure 2c). Film **II** is observed visually after the completion of ten cycles (Figure 2c, inset). Films deposited on FTO by superoxide anion radical-initiated electrochemical process have a more pronounced colour intensity compared to films deposited by direct oxidation of porphyrin.

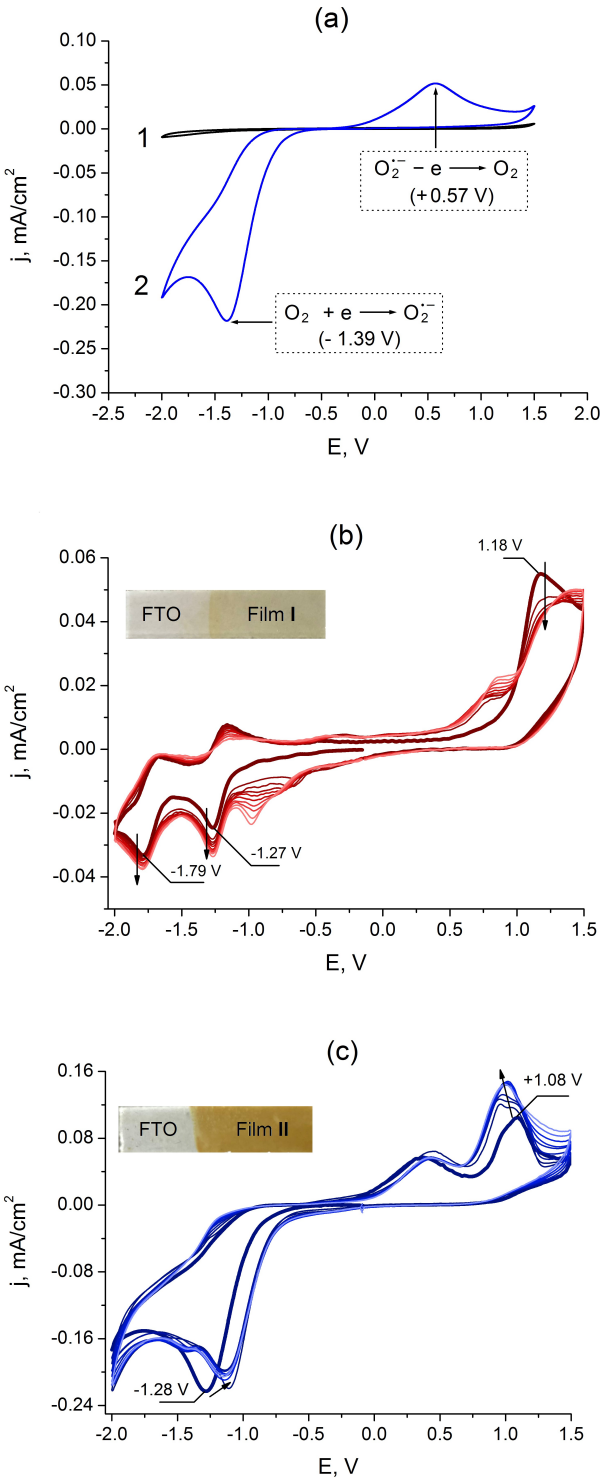

Figure 2. Electrochemical responses on the FTO electrode for: a) oxygen free (1) and oxygen saturated DMSO solutions (2); b) oxygen free 1mM CuT(3-NH_2Ph)P DMSO solution (10 cycles); c) oxygen saturated 1mM CuT(3- NH_2Ph)P DMSO solution (10 cycles).

Spectral properties

In the spectra of Film **I** and Film **II** (Figure 3a,b), there are bands characteristic to the molecular form of CuT(3-NH_2Ph)P: the Soret band with a maximum near 423 nm, and Q-bands with maxima at 543 and 620 nm. Compared to the spectrum of molecular porphyrin in solution, the spectra of the films exhibit an increase in the Soret band width (for Film **II** greater than for Film **I**). The relative intensity of the Q-band with a maximum at 620 nm in the spectra of the films is noticeably reduced. Broadening of lines in the spectrum is characteristic of porphyrins in the solid state. At this, the spectrum of the polymer may differ insignificantly from the spectrum of monomeric forms if the binding between the porphyrin fragments through the side substituent does not significantly change the electronic structure of the macrocycle.[36] The degenerate structure of the Q-band in the spectra of the films indicates the presence of a metal ion inside the macrocycle. The optical density in the films spectra (Figure 3b) characterizes the amount of material forming the film. Based on the optical density of films at the maximum of the Soret band, one can estimate the relative contribution of the mechanisms described in Scheme 1 to the film formation. Since the deposition duration of both Film **I** and Film **II** was similar, we can asses the relative efficiency of the two film formation mechanisms. Assuming that the presence of oxygen (superoxide) in solution does not significantly change the efficiency of the radical forms of porphyrin synthesis in electrooxidation processes (Scheme 1, reaction (a)), the difference in the optical densities of spectra 2 and 1 in Figure 2b one can attribute to the contribution of superoxide-initiated (Scheme 1, reaction (b)) film deposition. The relative contribution was calculated as the ratio of the obtained values of optical density. Thus, the study performed allowed us to quantify the relative efficiency for the two film formation mechanisms. In oxygenated solutions, the initiation of polymerization by superoxide exhibits a greater contribution to the film formation than the electrochemical oxidation of porphyrin does. The rates of film formation via these two mechanisms were found to differ by approximately three times.

In addition to the molecular lines of porphyrin fragments, the spectra of the films contain a region that can be attributed to the long-wave absorption edge of the semiconductor material (wavelengths lower than 370 nm) on the basis of the linearization in Tauck coordinates (Figure 3c,d). According to the modern understanding of the spectral characteristics of semiconductor materials, the spectral shape relates to the material's band gap.[37,38] This approach is widely used to analyze the characteristics of porphyrin-based materials.[37-41] In the present work it leads to the band gap values of 3.48 eV for Film **I** and 3.19 eV for Film **II**.

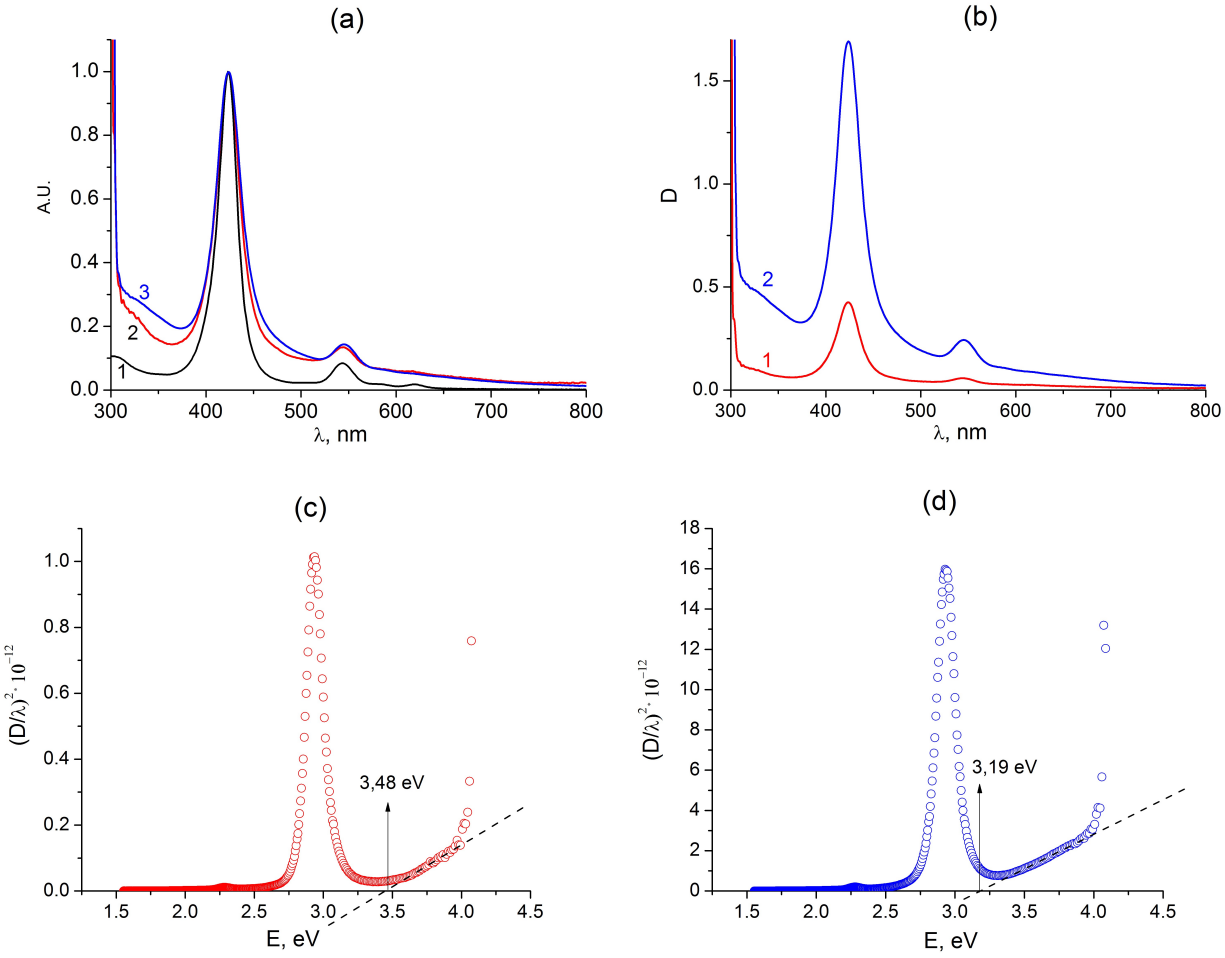

Figure 3. (a) Normalized spectra of DMSO solution of CuT(3-NH_2Ph)P (1), Film **I** (2) and Film **II** (3); (b) optical density of Film **I** (1) and Film **II** (2) on the FTO electrodes; (c) Tauc plot based on the Film **I** spectrum; (d) Tauc plot based on the Film **II** spectrum.

Surface morphology

The surface morphology at the microscopic level is determined by physicochemical phenomena occurring near the surface during film deposition, and largely determines the functional characteristics of the resulting material. According to the AFM study results (Figure 4, Table 1), the switching "on" the mechanism of superoxide-initiated polymerization leads to a significant change in the surface structure. The surface of the materials is formed by rounded globules with lateral dimensions of about 70 nm for Film **I** and about 50 nm for Film **II**. The surface images (Figure 4a,b,d,e) and the height distributions along the selected line (Figure 4c,f) indicate the formation of surface aggregates, which have a more complicated shape in the case of the Film **II**. The surface roughness of Film **II** is higher than that of Film **I**. The topographic images of the surface (Figure 4a,d) coincides with the phase contrast images (Figure 4b,e), which indicates the homogeneous surface composition of the resulting materials. According to the spectral characteristics (Figure 3), the deposition rate of Film **II** is higher than that of Film **I**. It is well known that the limiting stage of film growth can be both the formation of nuclei of a new phase and the growth of the particles of the new phase.[42] So, the size of particles depends on the ratio of nucleation and growth rates. The smaller size of the surface-forming particles for Film **II** indicates that in the case of turned "on" superoxide-initiated polymerization the increasing of nucleation rate is more pronounced than that of growth rate.

Table 1. Roughness parameters of the Film **I** and Film **II.** The data are collected from the surface areas of 5×5 μm.

Parameter, nm	Film **I**	Film **II**
Average Lateral size of surface particles	70	50
Peak-to-peak, Sy	103.7	123.7
Ten point height, Sz	51.6	61.7
Average Roughness, Sa	10.7	14.3
Root Mean Square, Sq	13.1	18.0

Oxygen reduction reaction (ORR)

Polymer films of porphyrins, obtained by polymerization initiated by electrochemical oxidation[23,26] and via the interaction of porphyrin with superoxide,[23,26,43] can potentially exhibit catalytic properties in the oxygen reduction reaction.[10,25,44,45] To reveal the possible catalytic activity of the obtained materials, the electrochemical response of oxygen electroreduction on a carbositall electrode was compared to that of the carbositall electrodes covered with Film **I** and Film **II** (Figure 5a,b). The potential for the onset of oxygen electroreduction on the electrodes under study differs slightly. At the same time, in the region of low overvoltages, the value of ORR current density increases in a row: carbositall < Film **I** < Film **II**. A current density of 0.2 mA/cm^2 is achieved at a potential of -0.302 V on carbositall, -0.296 V on Film **I**, and -0.284 V on Film **II**. The kinetic control region of the electrochemical process presented in Tafel coordinates (Figure 5b) demonstrates a decrease in its slope in the same row: carbositall < Film **I** < Film **II**. The Tafel slope values were 0.153, 0.146, and 0.130 V/dec for carbositall, Film **I** and Film **II**, consequentially. Decrease of the slope in Tafel coordinates, as a rule, points at the rise in the rate of the kinetic stage of electrochemical reaction.

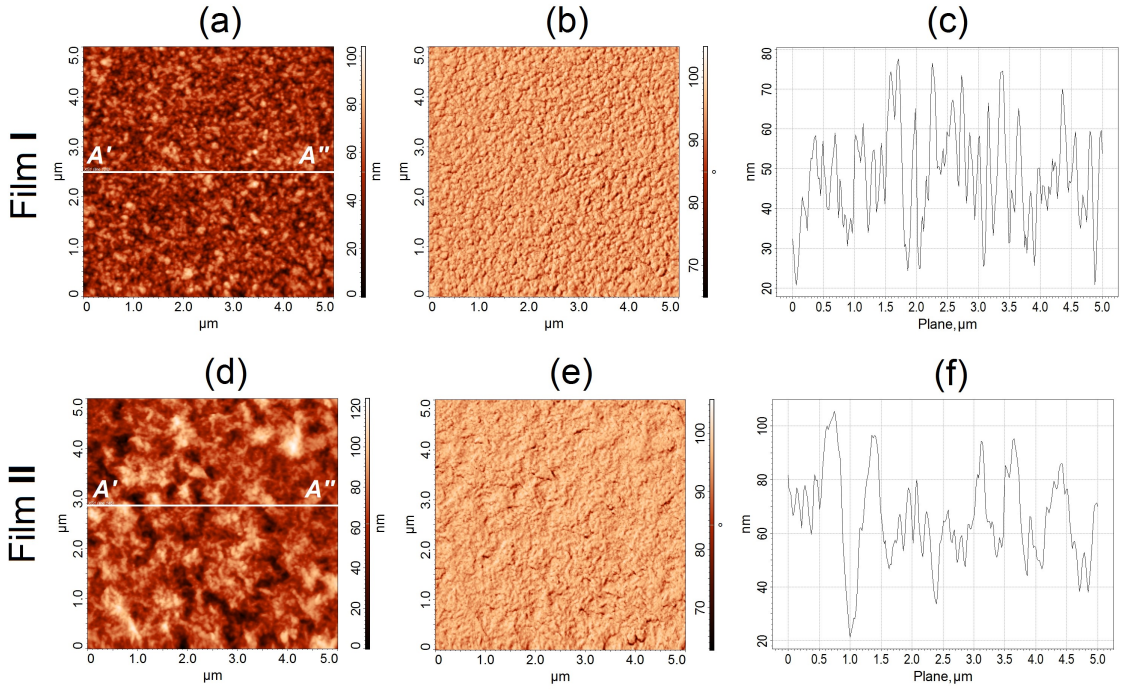

Figure 4. AFM images of the surface of Film **I** and Film **II** films: topography mode (a, d); phase contrast mode (b, e); distribution of film surface heights along line A'A'' (c, f). The scanning area is 5×5 μm.

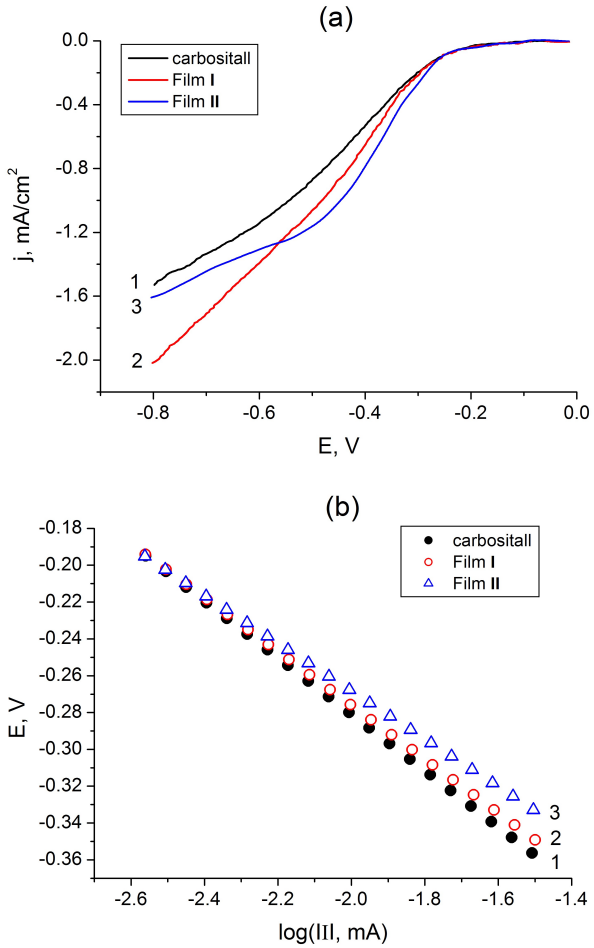

Figure 5. LSV of oxygen electroreduction (a) and Tafel slopes (b) on carbositall (1), on Film **I** (2) and Film **II** (3) in oxygen-saturated 0.1 M KOH. Rotation speed 500 rpm. Potential sweep rate 10 mV/s.

Conclusions

The study of the formation of films based on CuT(3-NH_2Ph)P from solutions in dimethyl sulfoxide allowed us for the first time to reveal that two different mechanisms of polymerization initiation coexist in oxygen-saturated solutions. An interesting finding is that the CuT(3-NH_2Ph)P films thick enough to study their physicochemical and practical properties can be obtained by electrooxidation of porphyrin in oxygen free DMSO. Comparison of the characteristics of the films obtained at turned "on" or "off" superoxide-initiated polymerization develops our understanding of the mechanisms of the processes, and of the relationship between the conditions of films formation and their properties. The work in this direction will allow us to approach the creation of materials with desired properties.

Acknowledgements. The work was supported by the Russian Science Foundation, project No. 24-13-00010. The authors express their gratitude to the group of Prof. S.A. Syrbu for the methodology of synthesis, purification and verification of porphyrins and the Upper Volga Region Centre of Physico-Chemical Research (G.A. Krestov Institute of Solution Chemistry of the Russian Academy of Sciences) for the equipment provided. The sited references (Electrochem. Commun. 2017, Mendeleev Commun. 2020, Russ. Chem. Bull. 2022, J. Electroanal. Chem. 2022, and Electrochim. Acta 2024) show the useful collaboration of O. I. Koifman with our group.

References

1. Kokorin M.S., Bazanov M.I., Semeikin A.S., Zheltova E.A., Berezina N.M. *Macroheterocycles* **2023**, *16*, 63–70. https://doi.org/10.6060/mhc224684b
2. Burmistrov V.A., Aleksandriiskii V.V., Novikov I.V., Pechnikova N.L., Shilov I.V., Lyubimtsev A.V., Ageeva T.A., Koifman O.I. *ChemChemTech* **2023**, *66*(7), 31–51. https://doi.org/10.6060/ivkkt.20236607.6832j
3. Berezina N.M., Bazanov M.I., Maizlish V.E. *Russ. J. Electrochem.* **2018**, *54*, 873-878. http://dx.doi.org/10.1134/S1023193518130074
4. Berezina N.M., Bazanov M.I., Semeikin A.S., Glazunov A.V. *Russ. J. Electrochem.* **2011**, *47*, 42–46. http://dx.doi.org/10.1134/ S1023193511010046
5. Minh D.N., Berezina N.M., Bazanov M.I., Semeikin A.S., Glazunov A.V. *Macroheterocycles* **2015**, *8*, 56–64. http://dx.doi.org/10.6060/mhc140714b
6. Berezina N.M., Klueva M.E., Bazanov M.I. *Macroheterocycles* **2017**, *10*, 308–312. https://doi.org/10.6060/mhc170507b
7. Kuzmin S.M., Chulovskaya S.A., Tesakova M.V., Koifman O.I., Parfenyuk V.I. *Electrochim. Acta* **2024**, *484,* 144025. https://doi.org/10.1016/j.electacta.2024.144025
8. Armijo F., Goya M.C., Reina M., Canales M.J., Arévalo M.C., Aguirre M.J. *J. Mol. Catal. A: Chem.* **2007**, *268*, 148–154. https://doi.org/10.1016/j.molcata.2006.11.055
9. Kuzmin S.M., Chulovskaya S.A., Dmitrieva O.A., Mamardashvili N.Z., Koifman O.I., Parfenyuk V.I. *J. Electroanal. Chem.* **2022**, *918,* 116476. https://doi.org/10.1016/ j.jelechem.2022.116476
10. Kuzmin S.M., Chulovskaya S.A., Parfenyuk V.I., Koifman O.I. *Mendeleev Commun.* **2020**, *30*, 777–780. https://doi.org/10.1016/ j.mencom.2020.11.030
11. Solovieva A., Vstovsky G., Kotova S., Glagolev N., Zav'yalov B.S., Belyaev V., Erina N., Timashev P. *Micron* **2005**, *36*, 508–518. https://doi.org/10.1016/j.micron.2005.05.004
12. Lee H., Park H., Ryu D.Y., Jang W.D. *Chem. Soc. Rev.*, **2023**, *52*, 1947–1974. https://doi.org/10.1039/D2CS01066F
13. Magna G., Šakarašvili M., Stefanelli M., Giancane G., Bettini S., Valli L., Ustrnul L., Borovkov V., Aav R., Monti D., Di Natale, C., Paolesse R. *ACS Appl. Mater. Interfaces* **2023,** *15*, 30674–30683. https://doi.org/10.1021/acsami.3c05177
14. Macor K.A., Spiro T.G. *J. Am. Chem. Soc.* **1983**, *105,* 5601–5607. https://doi.org/10.1021/ja00355a012
15. Kuzmin S.M., Chulovskaya S.A., Koifman O.I., Parfenyuk V.I. *Electrochem. Commun.* **2017**, *83*, 28–32. https://doi.org/10.1016/ j.elecom.2017.08.016
16. Zaar F., Olsson S., Emanuelsson R., Strømme M., Sjodin M., *Electrochim. Acta* **2022**, *424,* 140616. https://doi.org/10.1016/ j.electacta.2022.140616
17. Arce R., delRío R., Ruiz-León D., Velez J., Isaacs M., delValle M.A., Aguirre M.J. *Int. J. Electrochem. Sci.* **2012**, *7*, 11596–11608. https://doi.org/10.1016/S1452-3981(23)16970-7
18. Schaming D., Ahmed I., Hao J., Alain-Rizzo V., Farha R., Goldmann M., Xu H., Giraudeau A., Audebert P., Ruhlmann L. *Electrochim. Acta* **2011**, *56*, 10454–10463. https://doi.org/10.1016/j.electacta.2011.02.064
19. Huo Z., Badets V., Bonnefont A., Boudon C., Ruhlmann L. *Comptes Rendus Chimie* **2021**, *24(S3),* 1–15. https://doi.org/10.5802/crchim.120

20. Kuzmin S.M., Chulovskaya S.A., Filimonova Y.A., Parfenyuk V.I. *J. Electroanal. Chem.* **2023,** *947*, 117798. https://doi.org/ 10.1016/j.jelechem.2023.117798
21. Filimonova Y.A., Chulovskaya S.A., Kuzmin S.M., Parfenyuk V.I. *ChemChemTech* **2023**, *66*(4), 35–42. https://doi.org/10.6060/ivkkt.20236604.6796
22. Tesakova M.V., Vikol L.K., Kuzmin S.M., Parfenyuk V.I. *ChemChemTech* **2022**, *65*(5), 58–67. https://doi.org/10.6060/ivkkt.20226505.6554
23. Kuzmin S.M., Chulovskaya S.A., Tesakova M.V., Semeikin A.S., Parfenyuk V.I. *J. Porphyrins Phthalocyanines* **2017**, *21,* 555-567. https://doi.org/10.1142/S1088424617500559
24. Kuzmin S.M., Chulovskaya S.A., Parfenyuk V.I. *Electrochim. Acta* **2022**, *425,* 140742. https://doi.org/10.1016/j.electacta. 2022.140742
25. Kuzmin S.M., Chulovskaya S.A., Parfenyuk V.I. *Electrochim. Acta* **2018**, *292*, 256–267. https://doi.org/10.1016/j.electacta. 2018.09.127
26. Tesakova M.V., Semeikin A.S, Parfenyuk V.I. *J. Porphyrins Phthalocyanines* **2016**, *20*, 793–803. https://doi.org/10.1142/S1088424616500930
27. Chen S.M., Chen Y.L. *J. Electroanal. Chem.* **2004**, *573*, 277–287. https://doi.org/10.1016/j.jelechem.2004.07.014
28. Lucero M., Ramırez G., Riquelme A., Azocar I., Isaacs M., Armijo F., Förster J.E., Trollund E., Aguirre M.J., Lexa D. *J. Mol. Catal. A: Chem.* **2004**, *221*, 71–76. https://doi.org/10.1016/ j.molcata.2004.04.045
29. Day N.U., Wamser C.C. *J. Phys. Chem. C* **2017**, *121*, 11076–11082. https://doi.org/10.1021/acs.jpcc.7b01071
30. Managa M., Mgidlana S., Khene S., Nyokong T. *Inorg. Chim. Acta* **2020**, *511,* 119838. https://doi.org/10.1016/j.ica.2020.119838
31. Semeikin A.S., Koifman O.I., Berezin B.D. *Chem. Heterocyclic Comp*. **1986**, *22*, 629–632. https://doi.org/10.1007/BF00575244
32. Kuzmin S.M., Chulovskaya S.A., Parfenyuk V.I. *J. Electroanal. Chem*. **2023**, *943*, 117594. https://doi.org/10.1016/j.jelechem. 2023.117594
33. Walter M.G., Wamser C.C. *J. Phys. Chem. C* **2010**, *114*, 7563–7574. https://doi.org/10.1021/jp910016h
34. Sawyer D.T., Roberts J.L. *J. Electroanal. Chem.* **1966**, *12*, 90–101. https://doi.org/10.1016/0022-0728(66)80021-9
35. Fujinaga T., Isutsy K., Adachi T. *Bull. Chem. Soc. Jpn.* **1969**, *42*, 140–145. https://doi.org/10.1016/0013-4686(70)90014-9.
36. Schmitz R.A., Liddell P.A., Kodis G., Kenney M.J., Brennan B.J., Oster N.V., Moore T.A., Moore A.L., Gust D. *Phys. Chem. Chem. Phys*. **2014**, *16*, 17569e17579. https://doi.org/10.1039/ C4CP02105C
37. Tauc J. *Amorphous and Liquid Semiconductors*. Plenum Press, NewYork, **1974**.
38. Nawar A.M., Makhlouf M.M. *J. Electron. Mater.* **2019**, *48*, 5771–5784. https://doi.org/10.1007/s11664-019-07359-4
39. Shehata M.M., Kamal H., Hasheme H.M., El-Nahass M.M., Abdelhady K. *Opt. Laser. Technol.* **2018**, *106*, 136–144. https://doi.org/10.1016/j.optlastec.2018.03.032
40. El-Nahass M.M., El-Deeb A.F., Metwally H.S., El-Sayed H.E.A., Hassanien A.M. *Solid State Sci.* **2010**, *12*, 552–557. https://doi.org/10.1016/j.solidstatesciences.2010.01.004
41. El-Nahass M.M., Ammar A.H., Atta A.A., Farag A.A.M., El-Zaidia E.F.M. *Opt. Commun.* **2011**, *284*, 2259–2263. https://doi.org/10.1016/j.optcom.2010.12.032
42. Lukomsky Yu.Ya., Gamburg Yu.D. *Physico-Chemical Foundations of Electrochemistry.* Dolgoprudny: Intellect, **2013**. 448 pp. [Лукомский Ю.Я., Гамбург Ю.Д. *Физико-химические основы электрохимии: учебное пособие.* Долгопрудный: Интеллект, **2013**. 448 с.].
43. Parfenyuk V.I., Kuzmin S.M., Chulovskaya S.A., Koifman O.I. *Russ. Chem. Bull.* **2022**, *719*, 1921–1929. https://doi.org/10.1007/s11172-022-3610-3
44. Kuzmin S.M., Chulovskaya S.A., Parfenyuk V.I. *J. Porphyrins Phthalocyanines* **2022**, *26,* 748–754. https://doi.org/10.1142/ S1088424622500572
45. Tesakova M.V., Lutovac M., Parfenyuk V.I. *J. Porphyrins Phthalocyanines* **2018**, *22,* 1047–1053. https://doi.org/10.1142/ S108842461850102X

Received 31.05.2024
Accepted 08.08.2024